N O T I C E

THIS DOCUMENT HAS BEEN REPRODUCED FROM MICROFICHE. ALTHOUGH IT IS RECOGNIZED THAT CERTAIN PORTIONS ARE ILLEGIBLE, IT IS BEING RELEASED IN THE INTEREST OF MAKING AVAILABLE AS MUCH INFORMATION AS POSSIBLE

NASA

Technical Memorandum 80696

Observations of Electron Gyroharmonic Waves and the Structure of the Io Torus

T. J. Birmingham, J. K. Alexander, M. D. Desch, R. F. Hubbard and B. M. Pedersen

MAY 1980

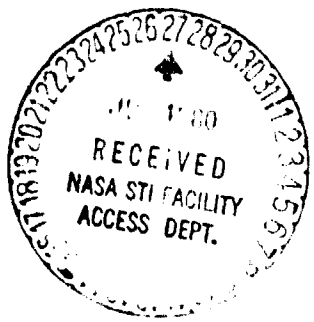

National Aeronautics and Space Administration

Goddard Space Flight Center
Greenbelt, Maryland 20771

OBSERVATIONS OF ELECTRON GYROHARMONIC WAVES AND THE STRUCTURE OF THE IO TORUS

T. J. Birmingham,[1] J. K. Alexander,[1] M. D. Desch,[2]
R. F. Hubbard,[3] B. M. Pedersen[4]

1. Laboratory for Extraterrestrial Physics, Goddard Space Flight Center, Greenbelt, Maryland 20772

2. Astronomy Program, University of Maryland, College Park, Maryland 20742

3. JAYCOR, 205 S. Whiting Street, Alexandria, Virginia 22304

4. Observatoire de Paris, Section d'Astrophysique de Meudon, 92190 Meudon, France

ABSTRACT

Narrow-banded emissions were observed by the Planetary Radio Astronomy experiment on the Voyager 1 spacecraft as it traversed the Io plasma torus. These waves occur between harmonics of the electron gyrofrequency and are the Jovian analogue of electrostatic emissions observed and theoretically studied for the terrestrial magnetosphere. The observed frequencies always include the component near f_{uhr}, the upper hybrid resonant frequency, but the distribution of the other observed emissions varies in a systematic way with position in the torus. A detailed discussion of the observations is presented. A refined model of the electron density variation, based on identification of the f_{uhr} line, is also included. Spectra of the observed waves are analyzed in terms of the linear instability of an electron distribution function consisting of isotropic cold electrons and hot loss-cone electrons. The positioning of the observed auxiliary harmonics with respect to f_{uhr} is shown to be an indicator of the cold to hot temperature ratio T_C/T_H. It is concluded that this ratio increases systematically by an overall factor of perhaps 4 or 5 between the inner ($L \sim 5\ R_J$) and outer ($L \sim 9\ R_J$) portions of the torus. Other relevant plasma and spectroscopic data are discussed.

INTRODUCTION

The Planetary Radio Astronomy (PRA) experiments on the Voyager 1 and 2 spacecraft have observed a rich variety of emissions of Jovian origin (cf. Warwick et al., 1979a, b). Because the frequency range of the PRA instruments is generally above characteristic frequencies of the plasma through which the spacecraft are moving, most of the observations have been of electromagnetic waves which have propagated from a distant source. Characteristic plasma waves have usually fallen into the lower frequency range of the Plasma Wave Science (PWS) experiment, and a rich variety have been observed *in situ* by the PWS team (Scarf et al., 1979; Gurnett et al., 1979), particularly inside the magnetosphere of Jupiter (Kurth et al., 1979a).

Within 10 R_J of Jupiter, the magnetic field is strong enough that the

electron gyrofrequency f_g climbs into the PRA range. Furthermore, plasma of possible Ionian origin--the Io plasma torus (IPT)--is sufficiently dense that the electron plasma frequency f_p exceeds f_g. In the IPT the PRA experiment on Voyager 1 observed a series of emissions which have been identified as locally generated electrostatic waves.

These electrostatic waves are narrow banded emissions which occur between harmonics of f_g and are generically related to waves observed by many earth-orbiting spacecraft (e.g., Kennel et al., 1970; Mosier et al., 1973; Shaw and Gurnett, 1975; Anderson and Maeda, 1977; Christiansen et al., 1978; Kurth et al., 1979b). They are commonly termed "gyroharmonic" or "n + 1/2" waves, although their frequencies may occur anywhere in the intervals between integral harmonics of f_g. They include strong emissions at the upper hybrid frequency f_{uhr}. Theory developed for the terrestrial observations has been applied in a preliminary analysis of the Voyager 1 results and has enabled the PRA team (Warwick et al., 1979a) to construct a model of the electron density variation through the torus.

The purposes of the present paper are (1) to present a more thorough description of the (n + 1/2) wave morphology within the IPT as seen by Voyager 1 and (2) based on these observations, to present results of a detailed application of theory.

The most striking feature of the Voyager 1 data in the IPT is a strong, bursty emission which has been interpreted as upper hybrid resonance noise (Warwick et al., 1979a). In addition there may be multiple banded (n + 1/2) waves above and/or below the upper hybrid band. A particular combination of observed waves seems to be characteristic of a particular portion of the torus, although one must be careful in using data from a single spacecraft pass which mixes radial, latitudinal, longitudinal and possibly temporal variations. The waves are analyzed in terms of the two component--hot and cold--electron stability analysis which has been carried out by several groups (Fredricks, 1971; Young et al., 1973; Young, 1975; Karpman et al., 1975; Ashour-Abdalla and Kennel, 1978; Hubbard and Birmingham, 1978; Ronnmark et al., 1978; Ashour-Abdalla et al., 1979) in conjunction with terrestrial studies. We conclude that the waves have important information, not only on

the total electron density, but on its bifurcation into cold and hot component and on the variation, as each type of wave is encountered, of the relative temperatures of the two.

Most of the electrons in the torus would appear from our analysis to be in the cold component, which may have a temperature $T_c < 10$ eV. Our interpretation of the electron variation, along with other observations which provide information from which electron density and temperature can be inferred, is complementary to the direct measurement of electrons (Scudder and Sittler, 1980) by the plasma instrument (Bridge et al., 1979). Electron measurements are important to the understanding of the chemical kinetics of the torus.

We shall not be discussing Voyager 2 results and interpretation. Voyager 2 had a Jovicentric distance at closest approach of 10.1 R_J and hence encountered only the outer fringe of the IPT.

OBSERVATIONS

The PRA experiment (Warwick et al., 1979a) measures right and left circularly polarized components of radiation and operates in two frequency bands. The high frequency band covers the range from 1.3 MHz to 40.5 MHz and is much above the characteristic frequencies of that portion of the Jovian magnetosphere traversed. Observations shown here were made in the low frequency band in which the receiver step-tunes at intervals of 19.2 kHz over 70 channels of bandwidth 1 kHz ranging from 1.2 kHz to 1.3 MHz. Each frequency sweep takes 6 seconds.

Shown in Figure 1 are the intensities, on a logarithmic scale, in several of the lower frequency channels for each 6 second interval. Over this time period Voyager 1 was outward bound through the IPT, moving from a Jovicentric distance of 6.5 R_J to 9.5 R_J. The electron gyrofrequency and several of its harmonics as determined from the onboard magnetometer experiment (Ness et al., 1979) are superposed.

This segment graphically illustrates the appearance of waves in the PRA

data, although as we shall see shortly there are several variations with position in the IPT of the precise frequency distribution pattern. Over this portion of the torus, steady, low intensity waves are observed in the 3/2, 5/2 and 7/2 frequency intervals. The 9/2 or 11/2 interval is generally characterized by the occurrence of the most intense and sporadic emission, which is identified from the theory as occurring at or near the upper hybrid resonance frequency $f_{uhr} = (f_{pc}^2 + f_g^2)^{1/2}$. (To be precise, the theory predicts that only the cold plasma density is to be used in calculating this f_{uhr}, but theory also predicts that whenever the upper hybrid emission is intense and bursty, as it is here, the plasma is dominantly cold and $f_{pc} \approx f_p$.) Over this portion of the IPT, waves are also seen in intervals above f_{uhr}; their appearance is less intense and bursty than the f_{uhr} emission but more so than the waves at low harmonics. Equal intensities are observed in both left and right polarizations so that these waves are probably either linearly polarized or unpolarized. As is the case for terrestrial observations no emission is ever seen in the 1/2 f_g regime. Since the PRA experiment is sensitive only to the electric component of the wave, these emissions cannot unambiguously be determined to be electrostatic. Our designation of them as such is based on their similarity with terrestrial waves, for which electric and magnetic measurements have been made (Shaw and Gurnett, 1975; Kurth et al., 1979b).

Figure 2 summarizes the occurrence of gyroharmonic waves for the entire Voyager 1 traversal of the IPT. Note that the f_{uhr} emission (filled circles) appears throughout the torus with the exception of a brief interval around closest approach (CA). We consider the positioning of the auxiliary $(n + 1/2)\ f_g$ emissions relative to the f_{uhr} line to be significant for determining variations in T_C/T_H, the cold to hot electron temperature ratio in the torus.

We believe that there are four distinct regimes in Figure 2: (1) the regime closest to Jupiter where the f_{uhr} emission occurs in the absence of auxiliary gyroharmonics, (2) a regime slightly farther out from Jupiter where the f_{uhr} line is accompanied by $(n + 1/2)\ f_g$ lines above it with either no lines or only one or two weak lines below, (3) a regime where half harmonic lines appear both above and below f_{uhr}, and finally, (4) a regime where f_{uhr}

is accompanied only by lower lying harmonics.

Figure 3 is a refined version of Figure 4 of the Warwick et al. (1979a) paper. The upper panel shows the density, determined from the identification of f_{uhr}, plotted as a function of time or equivalently position in the IPT. The lower panel is produced by smoothing of the upper panel density plot and transferring each point to the appropriate position along a meridional plot of the Voyager 1 trajectory. Additional data points are generated by assuming that the IPT possesses symmetry with respect to the particle centrifugal equator (Gledhill, 1967). This is a bit different from Warwick et al. (1979a), where the magnetic equator was used in this symmetrization process. Bagenal et al. (1980) and Cummings et al. (1980) have noted that for the relatively cold ions of the IPT the symmetry surface is the centrifugal equator rather than the magnetic equator. This situation should also apply to the IPT electrons, which, as we shall show below, are also predominantly cold. Of course, the assumption of longitudinal symmetry is also made here.

What is also new in Figure 3 is that the Voyager trajectory has been coded to indicate the type of gyroharmonic emission which has been observed. It will be our conclusion, based on the theoretical results of the next section, that the positioning of the four regimes as shown indicates that T_C/T_H becomes progressively larger as one moves outward in the torus, at least until one reaches the position where only f_{uhr} and lower frequency waves appear.

Our conclusions regarding the variation of T_C/T_H in the IPT are based on the comparison between measured electric wave power spectra and plots of electrostatic instability growth rates as a function of frequency. The next section will be devoted to a summary of the theory. We conclude here by showing measured spectra (Figures 4) representative of the emissions seen in the four regimes. The spectra, labelled A through D, were measured at the points designated in Figure 3 and are representative of the four regimes of the IPT. Tic marks at the top of each panel indicate the observing-to-electron gyrofrequency ratio, f/f_g. Every fifth tic mark is numbered. Since the bandwidth of the instrument is much less than f_g and the spacing between

adjacent channels is comparable with f_g, the relative intensities of different maxima in these plots are not always indicative of the relative intensities of the components of the actual emissions.

We begin with the regime nearest Voyager closest approach. Spectrum A, measured at 0935 SCET when Voyager 1 was at 5.6 R_J, is typical of conditions inside about L = 6. Only a single prominent f_{uhr} line is observed, in this case near 350 kHz, with no accompanying gyroharmonics. As the spacecraft moves into region B, (n + 1/2) line emission begins to appear above f_{uhr}. Figure 4b illustrates such a case, at 0818 SCET, in which no less than three (n + 1/2) super-harmonics are apparent. The spacecraft is at 6.4 R_J here. Notice that the intensity of the (n + 1/2) harmonics is a strong function of their proximity to the upper hybrid line. In region C, (n + 1/2) harmonics are prominent both above and below f_{uhr}, as evidenced here by Figure 4c. In this spectrum made at 1605 SCET and 6.5 R_J, four harmonics below and three above f_{uhr} are visible. As in Figure 4b, the super-harmonic proximate to f_{uhr} is the strongest (n + 1/2) line, with successively higher order lines decreasing in intensity. The harmonics below f_{uhr} appear to have equal power; however, this is an artifact of the sampling in frequency space. Reference to Figure 1 shows that in actuality the higher order sub-harmonics, i.e., those nearest f_{uhr}, are more intense. Finally, Figure 4d typifies the morphology we observe in the outer regions of the IPT, where $n_e \lesssim 500$ cm^{-3}. We illustrate it by a spectrum taken at 0532 SCET when Voyager is at 8.5 R_J. The f_{uhr} peak is at 136 kHz and no harmonic structure is apparent above f_{uhr}. Below f_{uhr}, however, three (n + 1/2) harmonics appear at approximately 9/2, 11/2, and 13/2 f_g. The individuality of the peaks is not as apparent here as previously because f_g is lower, reducing our effective frequency resolution. The harmonic identifications may be verified, however, by reference to time plots of the type shown in Figure 1.

Note again that the 19 kHz separation between adjacent PRA channels is a significant fraction of f_g and precludes definition of the shape of an emission line by several simultaneously observed frequency points. An estimate of the frequency width of a line may, however, be made by noting the passage of an emission peak in time through a given measurement channel owing to the spatially changing f_g. Assuming that the spectrum as a function of

f/f_g remains the same over the spatial interval traversed in tracing out the line, we estimate that the peaks in Figure 4 have a typical full width at half power of 10-20 kHz. The strongest emissions in Figure 4 have a spectral density of 10^{-13} V^2/m^2Hz and thus correspond to an integrated field strength of $\approx$ 30 $\mu V/m$. Such amplitudes are in the range of diffuse emissions seen in the earth's magnetosphere (Shaw and Gurnett, 1975) and are smaller by as much as an order of magnitude than the $(n + 1/2)$ f_g waves seen by the PWS experiment (Kurth et al., 1979a) tightly confined to the magnetic equator beyond 8 R_J in the Jovian magnetosphere. The latter are much akin to the Class 1 and Class 2 emissions (Hubbard and Birmingham, 1979) seen terrestrially. Despite this relatively weak intensity, the peaks in Figure 4 rise markedly above the surrounding noise level and are much more intense than the 10^{-16} V^2/m^2Hz electrostatic fluctuation level expected from a plasma of density $n \approx 10^3$ cm^{-3} and temperature $T \approx$ 1-10 eV (the value we infer from the results of the next section) in thermal equilibrium. This level is a rough estimate based on a calculation (Birmingham et al., 1965) which neglects the ambient magnetic field. It also neglects the interaction between the measuring antenna and the plasma (Meyer-Vernet, 1979), an effect which appears to play a significant role in low intensity solar wind measurments (Hoang et al., 1980). The strongest evidence in favor of a non-thermal origin is the significant enhancements over background and the sporadic nature of these bursts. We thus proceed to an instability explanation, acknowledging the possibility that these IPT waves may be a manifestation of a stable but non-thermal plasma differing but slightly from the weakly unstable characteristics which we attribute to it.

THEORETICAL RESULTS

We attribute the waves observed in the IPT to the instability of an electron plasma (with neutralizing ion background), consisting of hot and cold components, imbedded in a magnetic field. The electrons are described by the distribution function

$$f(V_\perp, V_{||}) = \frac{2}{\pi^2} \frac{1}{a_H} \frac{V_\perp^2}{(V_{||}^2 + a_H^2)^2} \exp - \frac{V_\perp^2}{a_H^2} + \frac{n_C}{n_H} \frac{1}{\pi^{3/2} a_C^3} \exp - \frac{V^2}{a_C^2} \qquad (1)$$

The hot electrons are represented by a Lorentzian parallel (to B) distribution with thermal width a_H and a Dory-Guest-Harris (1965) loss cone perpendicular distribution, also with thermal width a_H. The cold electrons have an isotropic Maxwellian distribution. The densities of the hot and cold components are n_H and n_C respectively and the normaliziation of f is such that $\int f d^3v = 1$ for the hot component alone.

Free energy for the instability derives from the loss cone nature of the hot electrons, while the cold plasma provides a dielectric background on which the unstable modes propagate. We have neglected in Eq. (1) provision for a fill-in hot component, which allows for the presence of hot electrons within the loss-cone ($V_\perp \gtrsim 0$) but still has a localized region of slope $\partial f/\partial V_\perp > 0$, conducive to instability. Such fill-in can alter the unstable spectrum quantitatively and qualitatively (cf. Fig. 8 of Hubbard and Birmingham, 1979) and is particularly effective in suppressing large n half harmonics. The fact that IPT waves have their strongest intensity at f_{uh}, where $n = 4$ or 5 (and large in the sense of Hubbard and Birmingham) thus argues against fill-in. The distribution given by Eq. (1) is amenable to an investigation in which a good deal of the work can be done analytically, but no claim is made that it is the only one which will produce $(n + 1/2) f_g$ unstable waves (Curtis and Wu, 1979). Several recent attempts have been made to examine terrestrial particle distributions made concurrently with wave observations. They have met with limited success in identifying phase space effects such as $\partial f/\partial V_\perp > 0$ which might be the cause of instability (Hubbard et al., 1979; Ronnmark, 1979; Kurth et al., 1979c).

As in Hubbard and Birmingham (1979) we investigate the stability of Eq. (1) by inserting it into the linear electrostatic dispersion relation. Cyclotron harmonic structure is found only in the waves propagating nearly perpendicularly to the magnetic field. We have concentrated on a regime

where all modes grow convectively. From our parametric search of unstable solutions to the electostatic dispersion relation we have found that it is only possible to excite dominantly the line in the upper hybrid harmonic interval if $n_C >> n_H$. Thus we conclude that through much of the IPT the cold plasma density greatly exceeds the hot density. The relative growth rates of different bands are, however, insensitive to the ratio n_C/n_H, as long as it is large, and hence it is not possible for us to specify this quantity exactly.

On the basis of our work, we do not go so far as to say that $n_C >> n_H$ throughout the IPT, for we have found it difficult to model Fig. 4d using convective instability alone. Whenever sub-harmonics appear in the theoretical results together with a strong f_{uhr} line, there are always super-harmonics.

The temperature ratio $T_C/T_H = a_C^2/a_H^2$ is, however, a more sensitive discriminator. Figures 5 exhibit the effect of varying this ratio in a situation where all other parameters are kept fixed. Plotted is the convective growth rate k_i, in units of inverse Larmor radii a_H/ρ_e of the hot component, against frequency f in units of the electron gyrofrequency f_g. For a given mode the convective growth rate k_i is related to the temporal growth γ_i by $k_i = \gamma_i/V_g$, were V_g is the group velocity. All plasma parameters with the exception of T_C/T_H have been held fixed in generating the solid curves in each panel: $n_C/n_H = 20$, $f_{uhr}/f_g = 7.73$, and $f_{ph}/f_g = 1.69$. (The gyrofrequency represents only a scale factor in this theory.) These same curves could have been produced (within a scale factor) by altering n_C/n_H (but keeping it large) and f_{ph}^2/f_g^2 in just the proper way to keep f_{uhr}/f_g at 7.73, hence the insensitivity to n_C/n_H.

As T_C/T_H is increased, first an emission above f_{uhr} appears and then additional emissions in lower interharmonic intervals. This is just the pattern exhibited by the observations through the first three regimes encountered in proceeding radially outward through the torus. We suggest that the radio observations are telling us that in addition to the cold plasma being much more dense than the hot, the temperature ratio T_C/T_H is increasing by a factor of roughly 2 in passing outward from regime to regime.

This may be due to a heating of the cold electrons, a cooling of the hot, or a combination of the two processes. For $T_C/T_H < .01$, the upper hybrid band becomes progressively more unstable, while growth in other bands, especially those above f_{uhr}, is suppressed. For $T_C/T_H > .04$, the growth of all elements in Fig. 5d is reduced, and additional bands above f_{uhr} appear.

The bottom two panels in Fig. 5 illustrate a nuance which is interesting and important in interpreting the data. While the upper hybrid line is generally the dominant unstable one, it is not necessarily always the case. In particular, when plasma parameters contrive to place f_{uhr} very close to a cyclotron harmonic nf_g, significant damping of the f_{uhr} line can ensue if the cold component is warm enough, as it is in the bottom panels of Figure 5. Under such circumstances it is the line in the next interval above f_{uhr} which grows dominantly. The dotted contours in panel 5c illustrate that by altering n_C and n_H slightly (but keeping $n_C/n_H = 20$) the f_{uhr} can be pushed far enough from the $f = 8\ f_g$ harmonic that dominance of the f_{uhr} line is restored.

Figures 6(a-c) show that we can explicitly reproduce the positions and relative strengths of the intensities shown in Figs. 4(a-c) with a two component electron plasma in which T_C/T_H varies from 0.01 to 0.04 in moving outward. As mentioned previously, we have had difficulty duplicating the characteristics of Figure 4d with purely convective modes. It may be necessary here to invoke absolute instabilities. Figure 5 of Kurth et al. (1979d) is certainly suggestive of this case and the value $T_C/T_H = 0.05$ which they use is in keeping with the outwardly increasing trend which we have found. However, in the terrestrial observatitons (Kurth et al., 1979d) (n + 1/2) emissions above f_{uhr} would be masked by electromagnetic continuum radiation. It is, therefore, not clear to us whether these terrestrial observations are the analogue of the Jovian emissions in Fig. 4(d) or whether they are really like Fig. 4(c). Kurth et al., (1979d) report no electrostatic waves above f_{uhr} in their modeling, but they may have neglected discussion of them because of the overriding presence of continuum in the observations.

One obvious and somewhat troubling aspect of the theory is that the

growth rate curves (Figures 5 & 6) are somewhat narrower in frequency than the observed logarithmic intensities. In the spirit of the present theoretical interpretation, which is that the unstable waves have exponentiated from thermal noise, one would expect the two to have comparable widths. A possible solution to the difficulty is that the electrostatic waves observed at a point may be the result of convective growth over a finite surrounding volume. If at each point of the volume, waves begin to grow at a frequency $f \simeq (n + 1/2)\, f_g(r)$ then a spread of $\simeq (n + 1/2)\, \Delta f_g(r) \simeq$ 10 kHz could be attained (for $n \approx 3$) if the contributing volume were typically 0.1 R_J in radial dimension.

Another possibility which is suggested by the recent work of Barbosa and Kurth (1979) is that our choice of electron distribution function has led to the narrow bands. These authors find significantly wider linear growth bands when they investigate the instability of an electron distribution which consists of a cold Maxwellian and a hot distribution which is power law in both energy and sine of the pitch angle. We cannot say, however, that use of the Barbosa and Kurth distribution would alter only the widths of our bands, leaving untouched all other correspondence between theory and observations.

COMPARISON OF JOVIAN AND TERRESTRIAL GYROHARMONIC WAVES

The theoretical model which was developed to explain terrestrial gyroharmonic waves can explain most features of the Jovian emissions in the Io plasma torus. In many ways, the waves which are observed in the terrestrial and Jovian magnetospheres are quite similar. Intense, bursty upper hybrid noise and somewhat weaker banded $(n + 1/2)$ emissions are observed at various times in both magnetospheres. Although the gyrofrequency in the IPT is higher than the earth's outer magnetosphere, the ratio f_p/f_g is typically 5-10 in both. The similarities in the wave emissions suggest that if the terrestrial emissions are indeed produced by a two-temperature electron plasma with $\partial f/\partial V_\perp > 0$ in part of the hot component, then similar electron distributions should exist in the IPT.

Nevertheless, there are important differences between the terrestrial and Jovian observations. The most common type of emission in the earth's

outer magnetosphere is the 3/2 wave, a single narrow band emission between f_g and 2 f_g. (The Class 1 emissions of Hubbard and Birmingham, 1978). Since f_{uhr} in this region lies well above 2 f_g in most cases, and since theory indicates that the emission should lie near the cold upper hybrid frequency (Ashour-Abdalla and Kennel, 1978; Hubbard and Birmingham, 1978), we conclude that the presence of such waves indicates that $n_C < n_H$.

Multiple (n + 1/2) emissions (Class 2 emissions) with no enhancement at the upper hybrid frequency are also a common feature of the earth's magnetosphere. Both theoretical models (Hubbard and Birmingham, 1978; Ashour-Abdalla et al., 1979) and the IMP 6 survey (Hubbard et al., 1979) indicate that such emissions are characteristic of somewhat larger cold plasma densities ($n_C/n_H \lesssim 1$). For $T_C/T_H \gtrsim 0.1$ all multiple cyclotron harmonic bands are usually convective, while at lower cold plasma temperatures, one or more of the bands may grow non-convectively (Ashour-Abdalla et al., 1979). For the IMP 6 cases examined by Hubbard et al. (1979), 3/2 or multiple gyroharmonic emissions (Classes 1 and 2) were accompanied by a plateau or peak in $f(V_\perp)$ in the 50-300 eV range, and T_C/T_H usually lay in the .05-.2 range assumed by Hubbard et al. (1979) and Ashour-Abdalla et al. (1979).

Although the Class 1 and Class 2 emission discussed above make up more than 80% of the IMP 6 observations, they never appear alone in the IPT. The upper hybrid resonance emission, however, appears throughout the torus. Similar emissions have been observed on several spacecraft in the earth's magnetosphere. Shaw and Gurnett (1975) reported narrow band emissions near the electron plasma frequency (which is near the upper hybrid resonance frequency for $f_p/f_g \gtrsim 3$ and $n_C >> n_H$). Hubbard and Birmingham (1978) termed these Class 4 emissions and showed that they could arise from the same theoretical model used to explain 3/2 emissions by setting $n_C/n_H >> 1$ and $T_C/T_H \sim .01$. Hubbard et al. (1979) surveyed IMP 6 data and showed that such emissions were indeed associated with large cold plasma densities. The most apparent source of free energy in the observed distribution function was a peak or plateau in $f(V_\perp)$ at a few keV.

More intense emissions near f_{uhr} were later reported by Kurth et al.

(1979b) just outside the terrestrial plasmapause. Such waves have now been observed on IMP 6 (Kurth et al., 1979b), Hawkeye 1 (Kurth et al., 1979b), ISEE 1 (Kurth et al., 1979d), and GEOS (Christiansen et al., 1978). Although much more intense than the emissions reported by Shaw and Gurnett (1975), they appear to be closely related theoretically. Kurth et al. (1979d) and Ronnmark et al., (1978) have used loss cone distribution with $n_C >> n_H$ for theoretical analysis of those waves. In addition, the distribution reported by Kurth et al. (1979d) during an upper hybrid event detected by ISEE 1 is very similar to that reported by Hubbard et al. (1979). The peak in the ISEE 1 distribution lies at a few keV, and only about .001 of the total electron density lies above the 200 eV lower energy limit of the detector, so that $n_C >> n_H$.

In addition to the intense upper hybrid band, one often sees one or two bands in adjacent super-harmonics in the earth's magnetosphere (Shaw and Gurnett, 1975; Hubbard and Birmingham, 1978). These are similar to the Voyager emission shown in Fig. 4b. Multiple harmonics in all bands leading up to the intense upper hybrid line are almost never seen in the data surveyed by Hubbard et al. (1979). However, such emissions are seen closer to the plasmapause (Kurth et al., 1979d) and are similar to the Voyager observations shown in Fig. 4c.

Based on the above discussion we conclude that the plasma in the IPT is similar in many respects to that found just outside the terrestrial plasmapause. Although the difference in gyrofrequency (and probably cold plasma temperature) introduces differences in scaling, the shape of f(V) is likely to be similar. We attribute the lack of single 3/2 emissions and the constant presence of upper hybrid noise in the IPT to having $n_C >> n_H$ everywhere in the torus.

DISCUSSION

The Voyager plasma experiment measured both ions and electrons in the energy range 10 eV to 5.9 keV (Bridge et al., 1979). In the IPT the instrument was capable of measuring corotating fluxes of ions with mass to charge ratio $A/Z \gtrsim 6$, and various charge states of sulfur (S) and oxygen (O)

were identified. The positive charge density associated with these ions agrees both in magnitude and radial variation (Bagenal et al., 1980) with the electron density plotted in Figure 3 and is the basis for the conclusion that the IPT contains mostly S and O ions.

The plasma experiment also measures ion temperatuare T_i in the IPT, especially well in the region $L < 6$ where the ions are coldest and thermal overlap of rotating distribution functions does not occur. A sharp outward radial gradient is observed, T_i (assumed the same for all ionic species) rising from $\sim$ 0.6 eV at $L \approx 5$ to $\sim$ 40 eV at $L \approx 6$. Beyond $L \approx 6$, T_i seems to level off or at least rise more slowly, but it is also difficult to measure T_i because of thermal overlap. The ion temperature gradient is in the same sense as the T_C/T_H gradient which we infer from the radio waves. However, it has a much shorter scale size and would appear to be concentrated toward smaller L-values.

The electron temperature in the outer Jovian magnetosphere measured in the hundreds of eV to several keV range (Krimigis et al., 1979; Bridge et al., 1979). Plasma electron results for the inner magnetosphere and the IPT are now available and confirm the two components, hot and cold, nature of the torus (Scudder and Sittler, 1980). Barbosa and Kurth (1979) have deduced a radial temperature variation from a theoretically determined radial pressure profile plus the measured electron density. The temperature so determined drops precipitously from a peak of $\sim$ 20 keV near $L \approx 20$ and may be 10 eV or less in the IPT. We conjecture that a two component, cold and hot, structure of electrons in the IPT is the result of mixing a dominant population of cold electrons, of possible Ionian origin, to a small density of hot (several hundred eV) electrons characteristic of the outer magnetosphere.

The S and O ions observed by the Voyager plasma experiment are the source of the extreme ultraviolet (EUV) line emissions seen by Broadfoot et al. (1979) in an experiment on the same spacecraft. A recent analysis (Strobel and Davis, 1980) suggests that the IPT electrons and ions are not in collisional ionization equilibrium (and hence brings into question how and if ion and electron temperatures in the IPT should be related). Rather "ionization rates determine the distribution of ionization states".

To model the observed EUV line intensities, Strobel and Davis have had to consider electron distributions with superthermal tails and have found a distribution consisting of a cold component of density 2000/cm^3 and energy 3.5-4 eV plus a hot component of density 50-100/cm^3 and energy $\sim$ 100 eV to be satisfactory. This model is completely compatible with our own.

The EUV measurements are made from a distance and integrate over the IPT. Ground based optical observations in both the lines of neutral sodium (NaI) and singly and doubly ionized sulfur (SII and SIII) have resolved radial structure. Both the NaI and SII (Mekler et al., 1979) emissions are confined largely to the portion of the torus inside of Io. These observations are consistent with the outer torus being richer in higher ionization states than the inner, the result presumably of impacts with hotter electrons.

A number of different Voyager observations--plasma, radio astronomy, and ultraviolet--have come from diverging approaches to common conclusions regarding the plasma of the IPT: the density is unexpectedly high; electrons are largely cold but there exists a small non-equilibrium admixture of hot electrons; and there is a radially outward gradient in the hot to cold temperature ratio of the two electron components. These conclusions are also consistent with ground based spectroscopic observations. Studies to the present have concentrated on gross understanding of the IPT. We expect that in the future greater attention will be paid to possible longitudinal or time dependent features such as the individual peaks and valleys in Fig. 3a. Electron spectra from the plasma experiment are now also becoming available (Scudder and Sittler, 1980). They indeed exhibit a two component electron structure. The interesting questions to be answered are whether the radio and other indirect interpretations of the IPT plasma require modification when they are constrained by observed details of the electrons such as their velocity and coordinate space structure.

ACKNOWLEDGMENTS

We are grateful to our colleagues from the Voyager Planetary Radio Astronomy team, especially A. Boischot, M. L. Kaiser, and J. W. Warwick, and

to J. D. Scudder of the Voyager Plasma Science team for many helpful discussions and to A. J. Dessler for a number of useful suggestions. We are particularly indebted to P. G. Harper for her assistance with the analysis and display of the data. One of us (B.M.P.) acknowledges the support of the French Space Research Organization (Centre National d'Etudes Spatiales).

REFERENCES

Anderson, R. R. and K. Maeda, VLF emissions associated with enhanced magnetospheric electrons, J. Geophys. Res., 82, 135, 1977.

Ashour-Abdalla, M. and C. F. Kennel, Nonconvective and convective electron cyclotron harmonic instabilities, J. Geophys. Res., 83, 1531, 1978.

Ashour-Abdalla, M., C. F. Kennel and W. Livesey, A parametric study of electron multiharmonic instabilities in the magnetosphere, J. Geophys. Res., 84, 6540, 1979.

Bagenal, F., J. D. Sullivan, and G. L. Siscoe, Spatial distribution of plasma in the Io torus, Geophys. Res. Lett., 7, 41, 1980.

Barbosa, D. D. and W. S. Kurth, Superthermal electrons and Bernstein waves in Jupiter's inner magnetosphere, U. of Iowa preprint 79-53, 1979.

Birmingham, T., J. Dawson, and C. Oberman, Radiation processes in plasmas, Phys. Fluids, 8, 297, 1965.

Bridge, H. S., J. W. Belcher, A. J. Lazarus, J. D. Sullivan, R. L. McNutt, F. Bagenal, J. D. Scudder, E. C. Sittler, G. L. Siscoe, V. M. Vasyliunas, C. K. Goertz, C. M. Yeates, Plasma observations near Jupiter: Initial results from Voyager 1, Science, 204, 987, 1979.

Broadfoot, A. L., M. J. S. Belton, P. Z. Takacs, B. R. Sandel, D. E. Shemansky, J. B. Holberg, J. M. Ajello, S. K. Atreya, T. M. Donahue, H. W. Moos, J. L. Bertaux, J. E. Blamont, D. F. Strobel, J. C. McConnell, A. Dalgarno, R. Goody, and M. B. McElroy, Extreme ultraviolet observations from Voyager 1 encounter with Jupiter, Science, 204, 979, 1979.

Christiansen, P. J., M. F. Gough, G. Martelli, J. J. Block, N. Cornilleau, J. Etcheto, R. Gendrin, C. Beghin, P. Decreau, and D. Jones, GEOS-1 observations of electrostatic waves, and their relationship with plasma parameters, Space Sci. Revs., 22, 383, 1978.

Cummings, W. D., A. J. Dessler, and T. W. Hill, Latitudinal oscillations of plasma within the Io torus, J. Geophys. Res., in press, 1980.

Curtis, S. A. and C. S. Wu, Electrostatic and electromagnetic gyroharmonic emissions due to energetic electrons in magnetospheric plasma, J. Geophys. Res., 84, 2057, 1979.

Dory, R. A., G. E. Guest and E. G. Harris, Unstable electrostatic plasma waves propagating perpendicular to a magnetic field, Phys. Rev. Lett., 14, 131, 1965.

Fredricks, R. W., Plasma instbility at (n + 1/2) f_c and its relationship to some satellite observations, J. Geophys. Res., 76, 5344, 1971.

Gledhill, J.A., Magnetosphere of Jupiter, Nature, 214, 155, 1967.

Gurnett, D. A., W. S. Kurth and F. L. Scarf, Plasma wave observations near Jupiter: Initial results from Voyager 2, Science, 206, 987, 1979.

Hoang, S., J.-L. Steinberg, G. Epstein, P. Tilloles, J. Fainberg, and R. G. Stone, The low frequency continuum as observed in the solar wind from ISEE 3: thermal electrostatic noise, to be published in J. Geophys. Res., 1980.

Hubbard, R. F. and T. J. Birmingham, Electrostatic emissions between electron gyroharmonics in the outer magnetsphere, J. Geophys. Res., 83, 4837, 1978.

Hubbard, R. F., T. J. Birmingham, and E. W. Hones, Jr., Magnetospheric electrostatic emissions and cold plasma densities, J. Geophys. Res., 84, 5828, 1979.

Karpman, V. I., Ju. K. Alekhin, N. D. Borisov, and N. A. Rjabova, Electrostatic electron-cyclotron waves in plasma with a loss-cone distribution, Plasma Phys., 17, 361, 1975.

Kennel, C. F., F. L. Scarf, R. W. Fredricks, J. H. McGehee, and F. V. Coroniti, VLF electric field observations in the magnetosphere, J. Geophys. Res., 75, 6136, 1970.

Krimigis, S. M., T. P. Armstrong, W. I. Axford, C. O. Bostrom, C. Y. Fan, G. Gloeckler, L. J. Lanzerotti, E. P. Keath, R. D. Zwickl, J. F. Carbary, and D. C. Hamilton, Low-energy charged particle environment at Jupiter: a first look, Science, 204, 998, 1979.

Kurth, W. S., D. D. Barbosa, D. A. Gurnett, and F. L. Scarf, Electrostatic waves in the Jovian magnetosphere, U. of Iowa preprint 79-46, 1979a.

Kurth, W. S., J. D. Craven, L. A. Frank, and D. A. Gurnett, Intense electrostatic waves near the upper hybrid resonance frequency, J. Geophys. Res., 84, 4145, 1979b.

Kurth, W. S., L. A. Frank, M. Ashour-Abdalla, D. A. Gurnett, and B. G. Burek, A free-energy source for intense electrostatic waves, U. of Iowa Preprint 79-36, 1979c.

Kurth, W. S., M. Ashour-Abdalla, L. A. Frank, C. F. Kennel, D. A. Gurnett, D. D. Sentman, and B. G. Burek, A comparison of intense electrostatic waves near f_{uhr} with linear instability theory, Geophys. Res. Lett., 6, 487, 1979d.

Mekler, Y., A. Eviatar, and G. L. Siscoe, Discontinuities in Jovian sulphur plasma, MNRAS, 189, 15 p., 1979.

Meyer-Vernet, N., On natural noises detected by antennas in plasmas, J. Geophys. Res., 84, 5373, 1979.

Mosier, S. R., M. L. Kaiser, and L. W. Brown, Observations of noise bands associated wih the upper hybrid resonance by the IMP-6 radio astronomy experiment, J. Geophys. Res., 78, 1673, 1973.

Ness, N. F., M. H. Acuna, R. P. Lepping, L. F. Burlaga, K. W. Behannon and F.

M. Neubauer, Magnetic field studies at Jupiter by Voyager 1: Preliminary results, Science, 204, 982, 1979.

Ronnmark, K., Electrostatic cyclotron waves in the magnetosphere, Univ. of Umea (Sweden) preprint 1979-03-26, 1979.

Ronnmark, K., H. Borg, P. J. Christiansen, M. P. Gough, D. Jones, Banded electron cyclotron harmonic instability - A first comparison of theory and experiment, Space Sci. Revs., 22, 401, 1978.

Scarf, F. L., D. A. Gurnett, and W. S. Kurth, Jupiter plasma wave observations: An initial Voyager 1 overview, Science, 204, 991, 1979.

Scudder, J. D. and E. C. Sittler, A survey of the plasma electron environment of Jupiter: direct measurements, J. Geophys. Res., this issue.

Shaw, R. R., and D. A. Gurnett, Electrostatic noise bands associated with the electron gyrofrequency and plasma frequency in the outer magnetosphere, J. Geophys. Res., 80, 4259, 1975.

Strobel, D. F. and J. Davis, Properties of the Io plasma torus inferred from Voyager EUV data, submitted to Ap. J. Lett., 1980.

Warwick, J. W., J. B. Pearce, A. C. Riddle, J. K. Alexander, M. D. Desch, M. L. Kaiser, J. R. Thieman, T. D. Carr, S. Gulkis, A. Boischot, C. C. Harvey and B. M. Pedersen, Voyager 1 planetary radio astronomy observations near Jupiter, Science, 204, 955, 1979a.

Warwick, J. W., J. B. Pearce, A. C. Riddle, J. K. Alexander, M. D. Desch, M. L. Kaiser, J. R. Theirman, T. D. Carr, S. Gulkis, A. Boischot, Y. Leblanc, B. M. Pedersen, and D. H. Staelin, Planetary radio astronomy observations from Voyager 2 near Jupiter, Science, 206, 991, 1979b.

Young, T. S. T., Destabilization and wave-induced evolution of the magnetosphere plasma clouds, J. Geophys. Res., 80, 3995, 1975.

Young, T. S. T., J. D. Callen, and J. E. McCune, High-frequency electrostatic waves in the magnetosphere, J. Geophys. Res., 78, 1082, 1973.

Figure 1. Intensity-time tracings of gyroharmonic lines in the IPT. Within each trace, identified by its frequency in kHz, the vertical dimension is logarithmically proportional to intensity. The variation in time of the electron gyrofrequency and its first nine integral harmonics is shown superposed.

Figure 2. Plot of the frequencies at which the Voyager 1 experiment detected narrow-band plasma wave lines during the traversal of the IPT. The solid dots denote the locations in frequency and time at which we observed intense impulsive emissions associated with the upper hybrid resonance frequency, and the open circles denote the occurrence of the relatively weaker and smoother $(n + 1/2)\ f_g$ emissions. The smooth curves show the locations of integral harmonics of the electron gyrofrequency derived from the magnetometer data of Ness et al. (1979).

Figure 3. (Upper panel) Plot of the density of the cold electron component of the IPT as a function of time derived from PRA measurements of the cold upper hybrid resonance frequency and magnetometer measurements of the electron gyrofrequency. The smooth curves in the regions of maximum density show how the data were smoothed to produce the model of electron density contours. (Lower panel) A model of the average density distribution in a meridional plane for the cold electron component of the IPT. The projection of the Voyager 1 trajectory through the IPT is coded to indicate the locations at which various classes of plasma wave lines were detected by the PRA instrument. Spectra observed at the points marked A, B, C, and D are shown in Figure 4.

Figure 4. Spectral density plots of gyroharmonic line emission in the IPT. Each plot is representative of a region in the torus characterized by a distinct line spectrum. See text for detailed description.

Figure 5. A plot of linear spatial growth rates as a function of wave frequency. All panels correspond to the same density composition n_C/n_H and with the exception of the dotted curve in (c) all have the same ratio $f_{uhr}/f_g = 7.73$ of upper hybrid resonance frequency to gyrofrequency.

Figure 6. Instability growth rates for the model electron distribution function Eq. (1), choosing $n_C/n_H = 20$. The parameters T_C/T_H and f_{uhr}/f_g have been adjusted so that growth in Figures 6 (a-c) occurs at the approximate frequencies and in proportion to the spectral densities shown in Figures 4(a-c). We have not been successful in so replicating the pattern of Figure 4d with a purely convective instability.

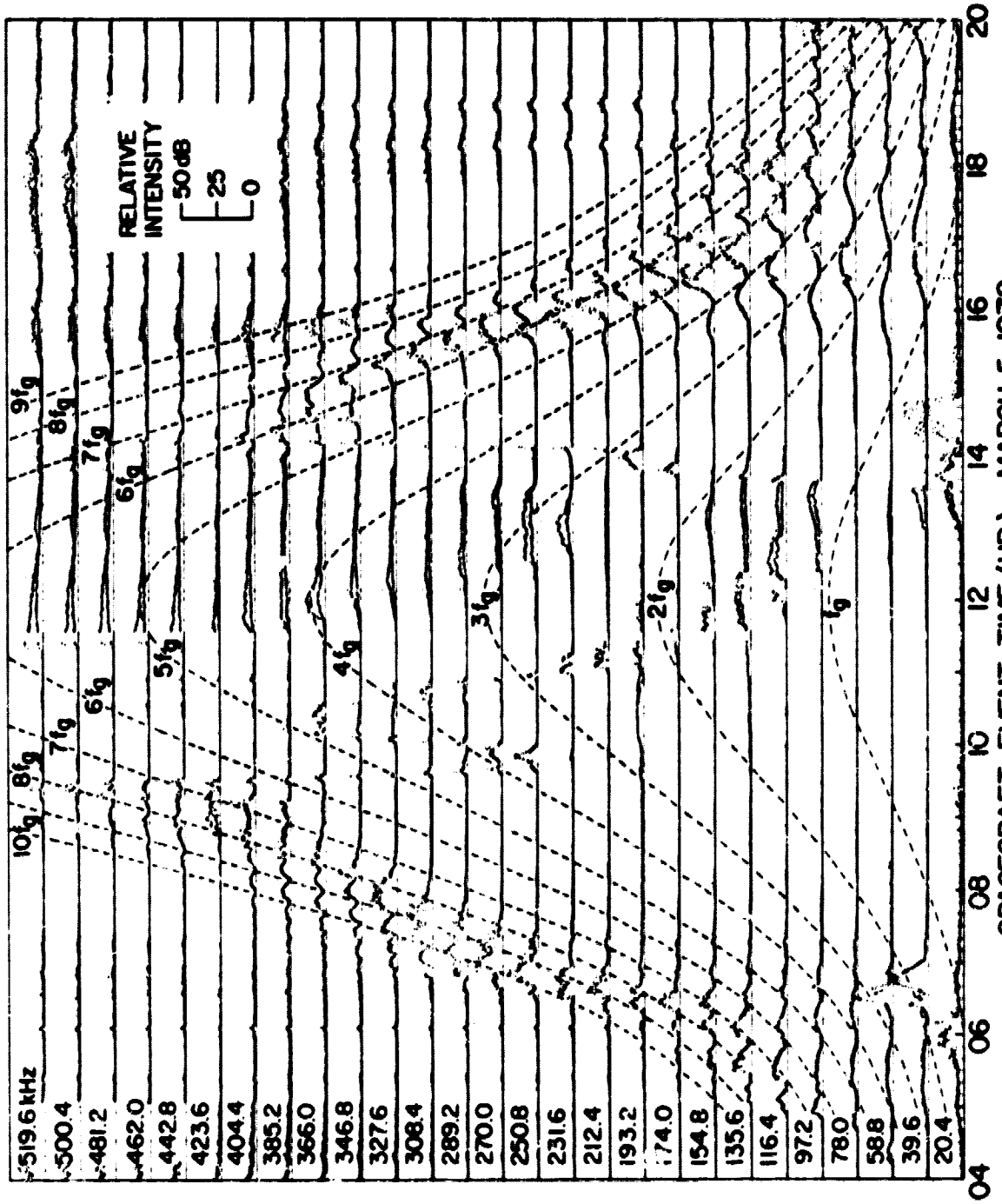

Fig. 1

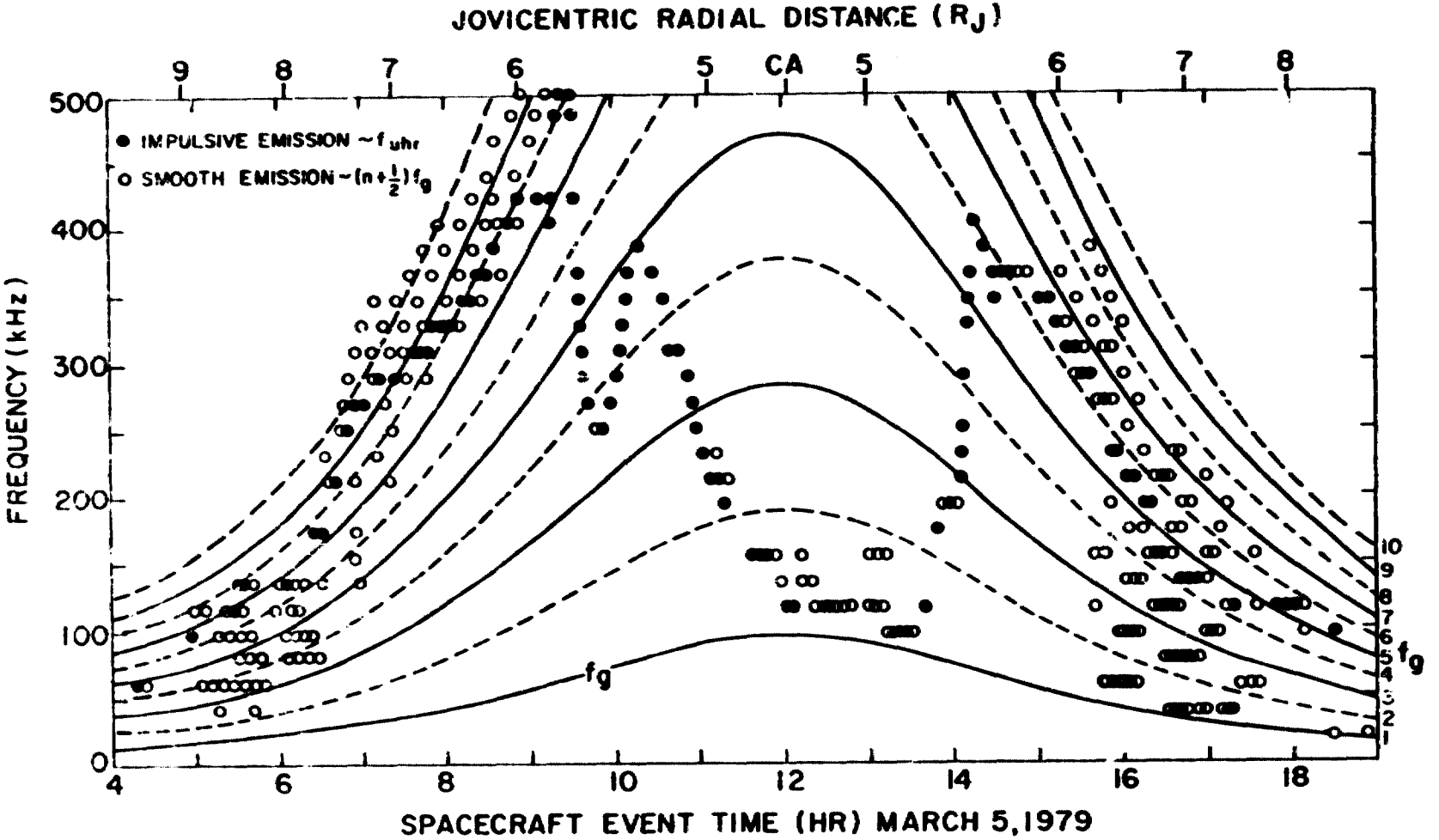
JOVICENTRIC RADIAL DISTANCE (R_J)
9
8
7
6
5
CA
5
6
7
8
500
400
300
200
100
0
FREQUENCY (kHz)
● IMPULSIVE EMISSION ~ f_{uhr}
○ SMOOTH EMISSION ~ $(n+\frac{1}{2})f_g$
f_g
10
9
8
7
6
5
4
3
2
1
f_g
4
6
8
10
12
14
16
18
SPACECRAFT EVENT TIME (HR) MARCH 5, 1979

Fig. 2

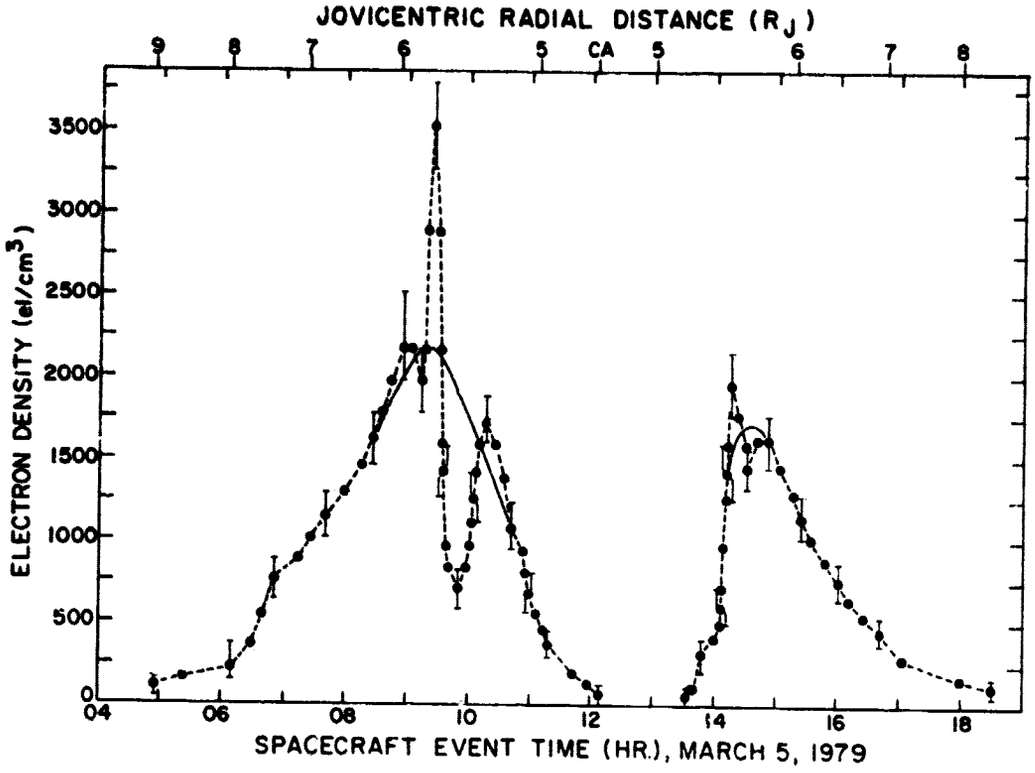

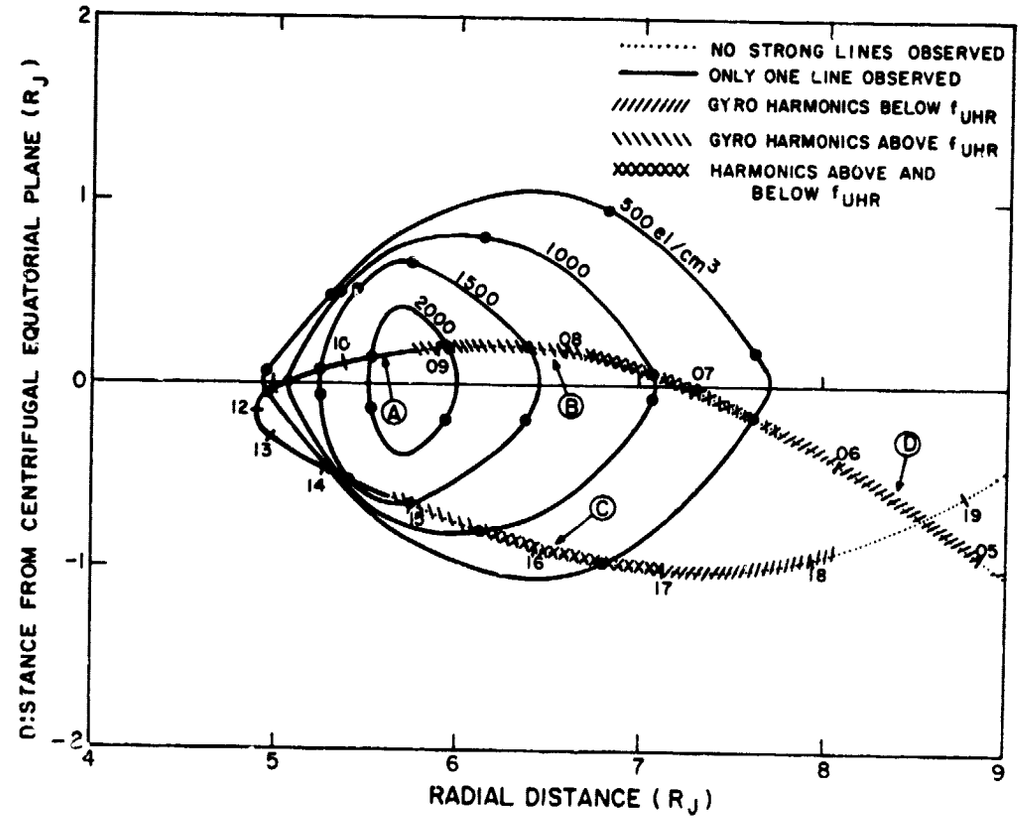

Fig.3

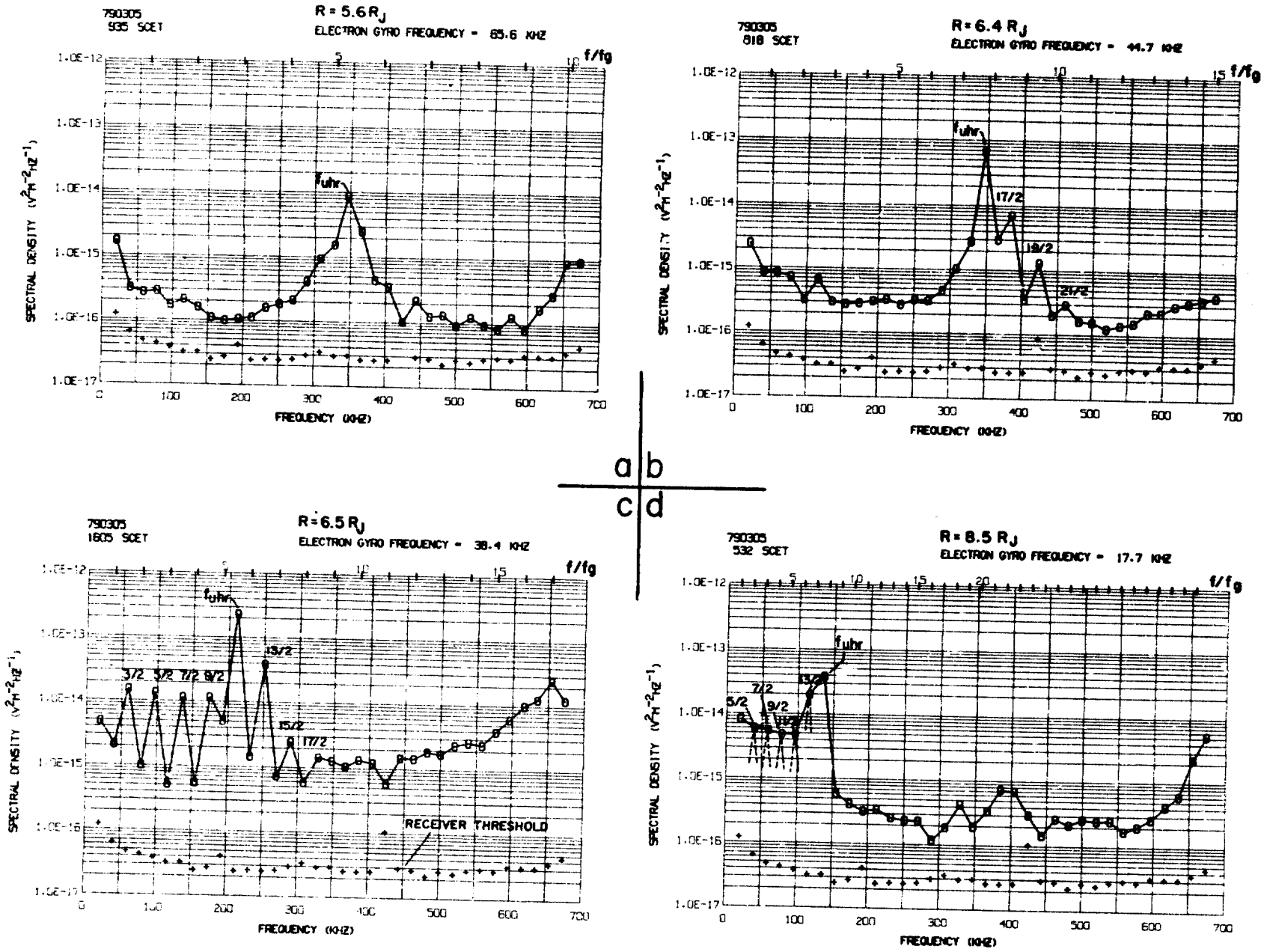
790305
935 SCET
R = 5.6 R_J
ELECTRON GYRO FREQUENCY = 65.6 KHZ
f/fg
SPECTRAL DENSITY (V²H⁻²Hz⁻¹)
FREQUENCY (KHZ)
f_uhr
790305
818 SCET
R = 6.4 R_J
ELECTRON GYRO FREQUENCY = 44.7 KHZ
17/2
19/2
21/2
790305
1605 SCET
R = 6.5 R_J
ELECTRON GYRO FREQUENCY = 38.4 KHZ
3/2 5/2 7/2 9/2
13/2
15/2
17/2
RECEIVER THRESHOLD
790305
532 SCET
R = 8.5 R_J
ELECTRON GYRO FREQUENCY = 17.7 KHZ
5/2
7/2
9/2
13/2
a b
c d

Fig. 4

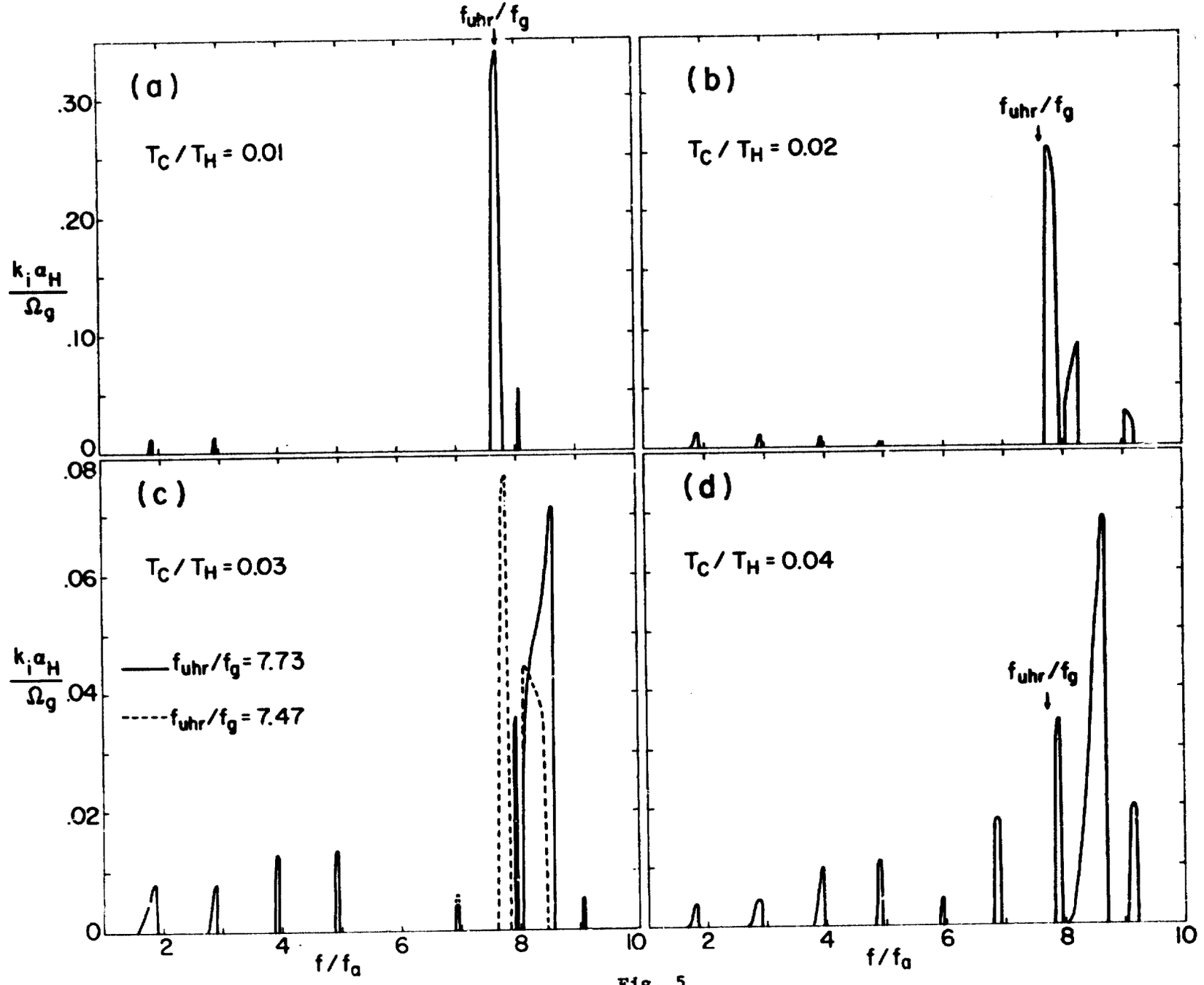
(a)
$T_C / T_H = 0.01$
f_{uhr} / f_g
(b)
$T_C / T_H = 0.02$
f_{uhr} / f_g
(c)
$T_C / T_H = 0.03$
$f_{uhr}/f_g = 7.73$
$f_{uhr}/f_g = 7.47$
(d)
$T_C / T_H = 0.04$
f_{uhr} / f_g
$\frac{k_i a_H}{\Omega_g}$
0
.10
.20
.30
.02
.04
.06
.08
2
4
6
8
10
f / f_a

Fig. 5

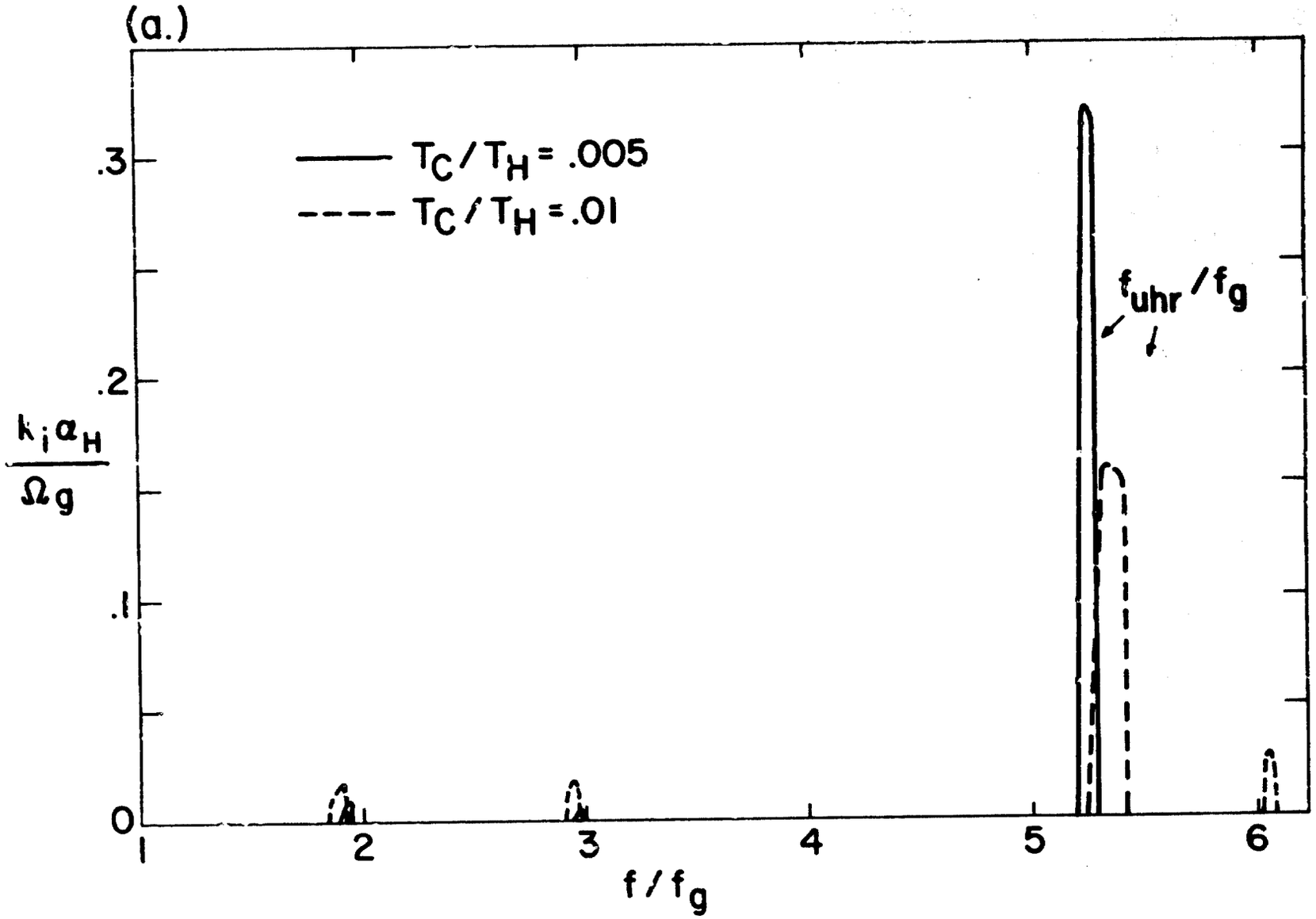
(a.)
$T_C/T_H = .005$
$T_C/T_H = .01$
f_{uhr}/f_g
$\frac{k_i \alpha_H}{\Omega g}$
.3
.2
.1
0
1
2
3
4
5
6
f/f_g

Fig. 6a

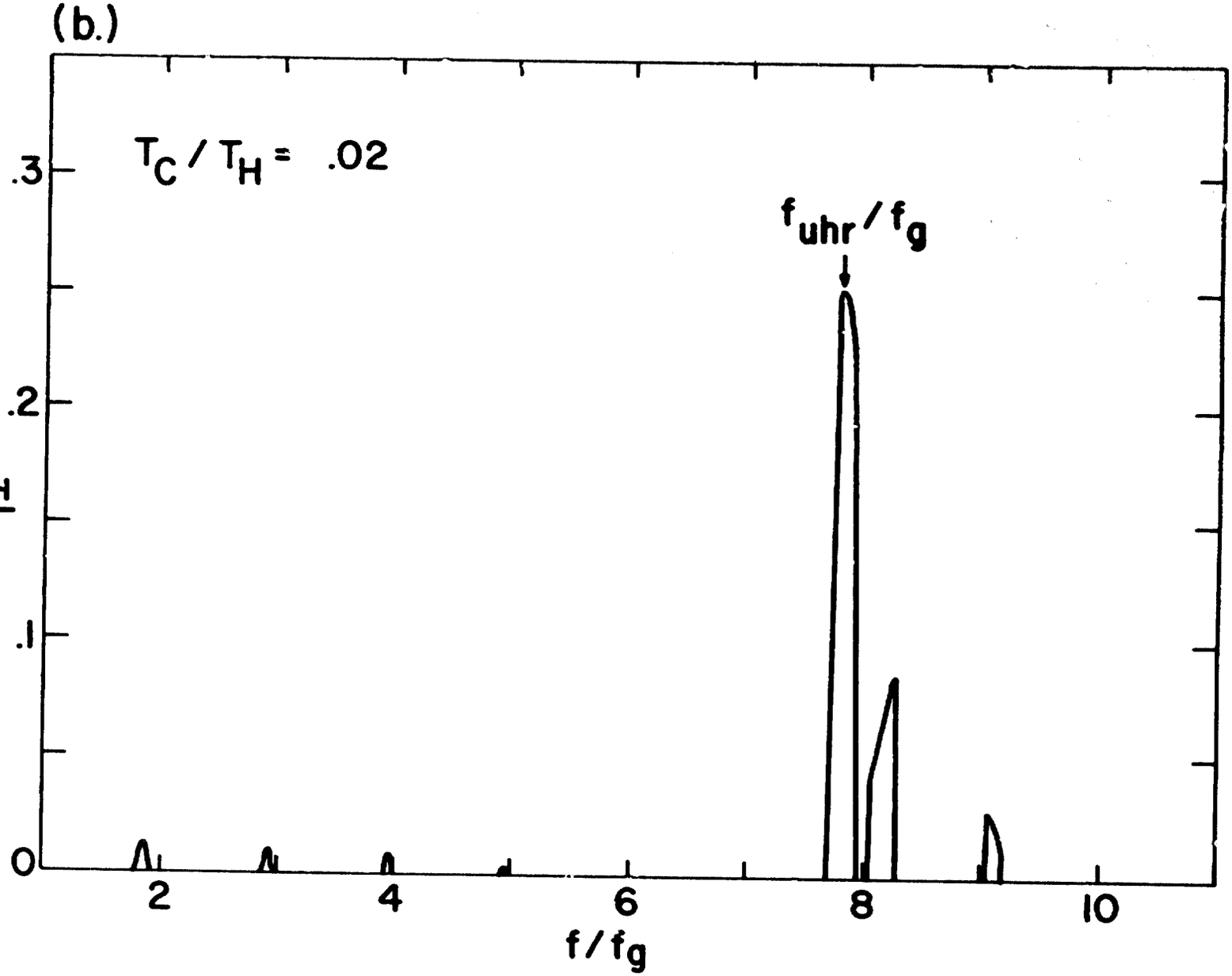

Fig. 6b

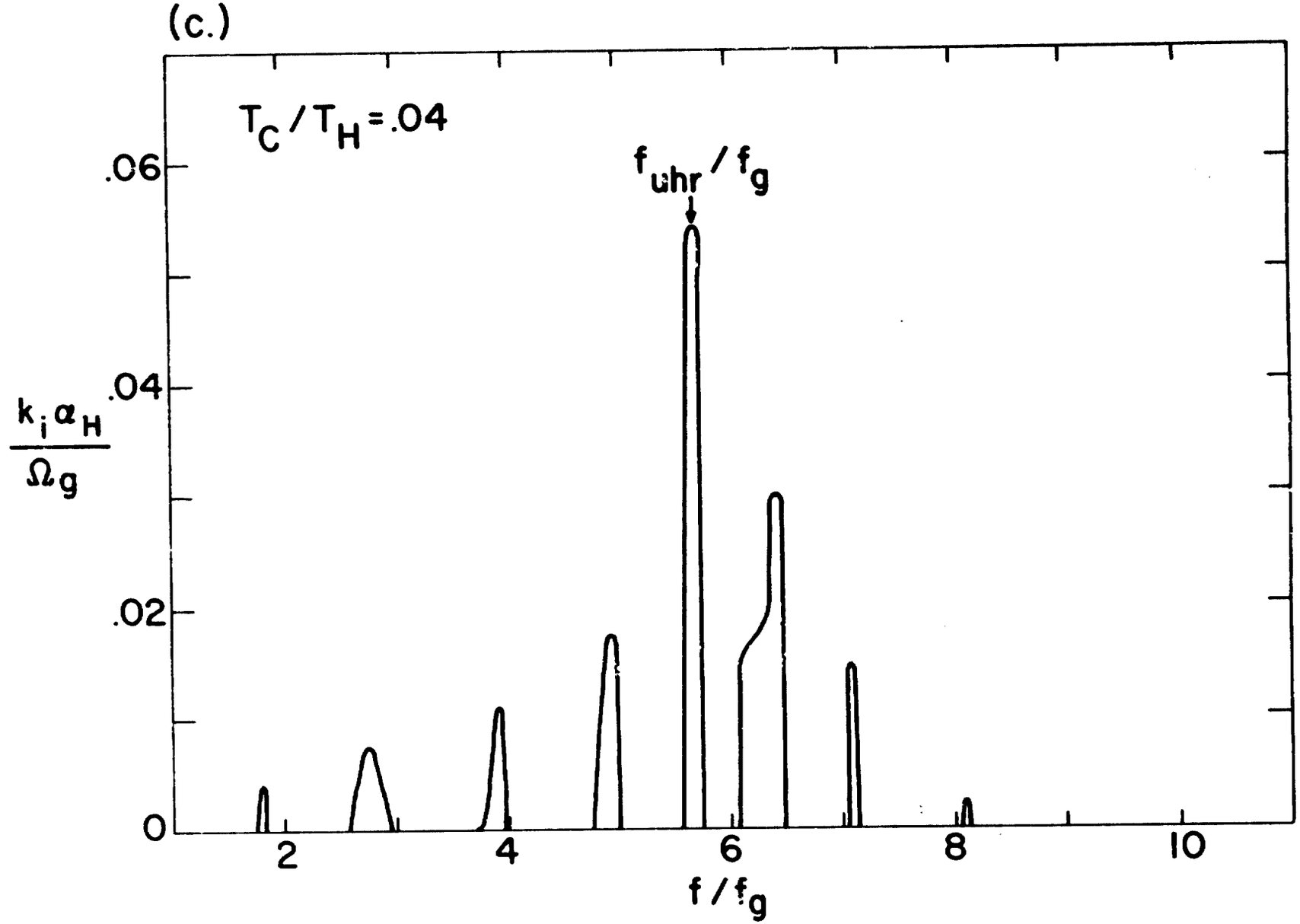

Fig. 6c

BIBLIOGRAPHIC DATA SHEET

1. Report No.	2. Government Accession No.	3. Recipient's Catalog No.
TM 80696		

4. Title and Subtitle	5. Report Date
Observations of Electron Gyroharmonic Waves and the Structure of the Io Torus	May 1980
	6. Performing Organization Code 695
7. Author(s) T. J. Birmingham, J. K. Alexander, M.D. Desch, R. F. Hubbard, B. M. Pedersen	8. Performing Organization Report No.
9. Performing Organization Name and Address Goddard Space Flight Center Greenbelt, Maryland 20771	10. Work Unit No. 11. Contract or Grant No.
12. Sponsoring Agency Name and Address	13. Type of Report and Period Covered Technical Memorandum
	14. Sponsoring Agency Code

15. Supplementary Notes

16. Abstract

Narrow-banded emissions were observed by the Planetary Radio Astronomy experiment on the Voyager 2 spacecraft as it traversed the Io plasma torus. These waves occur between harmonics of the electron gyrofrequency and are the Jovian analogue of electrostatic emissions observed and theoretically studied for the terrestrial magnetosphere. The observed frequencies alwyas include the component near f_{uhr}, the upper hybrid resonant frequency, but the distribution of the other observed emissions varies in a systematic way with position in the torus. A detailed discussion of the observations is presented. A refined model of the electron density variation, based on identification of the f_{uhr} line, is also included. Spectra of the observed waves are analyzed in terms of the linear instability of an electron distribution function concsisting of isotropic cold electrons and hot loss-cone electrons. The positioning of the observed auxiliary harmonics with respect to f_{uhr} is shown to be an indicator of the cold to hot temperature ratio T_C/T_H. It is concluded that this ratio increases systematically by an overall factor of perhaps 4 or 5 between the inner ($L \sim 5\ R_J$) and outer ($L \sim 9\ R_J$) portions of the torus. Other relevant plasma and spectroscopic data discussed.

17. Key Words (Selected by Author(s))	18. Distribution Statement
Jupiter magnetosphere, Voyager, Io plasma torus	

19. Security Classif. (of this report)	20. Security Classif. (of this page)	21. No. of Pages	22. Price*
U	U	30	

*For sale by the National Technical Information Service, Springfield, Virginia 22151.